



An *in vitro* pharmacogenomic approach reveals subtype-specific therapeutic vulnerabilities in atypical teratoid/rhabdoid tumors (AT/RT)

David Pauck ^{a,b,c,ip}, Daniel Picard ^{b,c,d}, Mara Maue ^{b,c}, Kübra Taban ^{b,c}, Viktoria Marquardt ^{b,c}, Lena Blümel ^{b,c}, Jasmin Bartl ^{b,c}, Nan Qin ^{e,f}, Nadezhda Kubon ^a, Dominik Schöndorf ^d, Frauke-Dorothee Meyer ^{b,c}, Johanna Theruvath ^{g,h}, Siddhartha Mitra ⁱ, Martin Hasselblatt ^j, Michael C. Frühwald ^{k,l}, Guido Reifenberger ^{a,c}, Marc Remke ^{b,c,d,*}

^a Institute of Neuropathology, Heinrich Heine University Düsseldorf, Medical Faculty, and University Hospital Düsseldorf, Düsseldorf, Germany

^b Department of Pediatric Oncology, Hematology and Clinical Immunology, Heinrich Heine University Düsseldorf, Medical Faculty, and University Hospital Düsseldorf, Düsseldorf, Germany

^c German Cancer Consortium (DKTK), partner site Essen/Düsseldorf, Düsseldorf, Germany

^d Pediatric Oncology and Hematology, Children's Hospital, Saarland University, Homburg, Germany

^e Clinic of Oncology, Hematology and Clinical Immunology, Heinrich Heine University Düsseldorf, Medical Faculty, and University Hospital Düsseldorf, Düsseldorf, Germany

^f Spatial & Functional Screening Core Facility, Heinrich Heine University Düsseldorf, Medical Faculty, Düsseldorf, Germany

^g Department of Neurosurgery, Institute for Stem Cell Biology and Regenerative Medicine and Division of Pediatric Neurosurgery, Lucile Packard Children's Hospital, Stanford University, Stanford, CA, USA

^h Stanford University School of Medicine, Stanford, CA, USA

ⁱ Pediatrics, University of Colorado Denver, Aurora, CO, USA

^j Institute of Neuropathology, University Hospital Münster, Münster, Germany

^k Pediatrics and Adolescent Medicine, Swabian Children's Cancer Center, University Hospital Augsburg and EU-RHAB Registry, Augsburg, Germany

^l Bavarian Cancer Research Center, Augsburg, Germany

ARTICLE INFO

ABSTRACT

Atypical teratoid/rhabdoid tumor (AT/RT) is a highly malignant embryonal brain tumor driven by genetic alterations inactivating the *SMARCB1* or, less commonly, the *SMARCA4* gene. Large-scale molecular profiling studies have identified distinct molecular subtypes termed AT/RT-TYR, -SHH and -MYC. Despite the increasing knowledge of AT/RT biology, curative treatment options are still lacking for certain risk groups and outcomes of these patients remain poor. We performed an *in vitro* high-throughput drug screen of 768 small molecule drugs covering conventional chemotherapeutic agents and late-stage developmental drugs in 13 AT/RT cell lines and determined intra- and inter-entity differential responses to unravel specific vulnerabilities. Our data demonstrated *in vitro* preferential activity of mitogen-activated protein kinase kinase (MEK) and mouse double minute 2 homolog (MDM2) inhibitors in AT/RT cell lines compared to other high-grade brain tumor cell lines including medulloblastoma and malignant glioma models. Moreover, we were able to link distinct drug response patterns to AT/RT molecular subtypes through integration of drug response data with large-scale DNA methylation and RNASeq-based expression profiles. Subtype-dependent drug response profiles demonstrated sensitivity of AT/RT-SHH cell lines to B-cell lymphoma 2 (BCL2) and heat shock protein 90 (HSP90) inhibitors, and increased activity of microtubule inhibitors, kinesin spindle protein (KSP) inhibitors, and the eukaryotic translation initiation factor 4E (eIF4E) inhibitor briciclib in a subset of AT/RT-MYC cell lines. In summary, our *in vitro* pharmacogenomic

Keywords:
Atypical teratoid/rhabdoid tumor
DNA methylation profiling
High-throughput drug screening
RNA sequencing
Targeted therapy

Chemical compounds studied in this article:
GDC-0623 (PubChem CID: 42642654)
idasanutlin (PubChem CID: 53358942)
ABT-737 (PubChem CID: 11228183)
ABT-199/venetoclax (PubChem CID: 49846579)
17-AAG/tanespimycin (PubChem CID: 6505803)
briciclib (PubChem CID: 11248490)

Abbreviations: BCL2, B-cell lymphoma 2; CAR, chimeric antigen receptor; CDK, cyclin-dependent kinase; DMSO, dimethyl sulfoxide; DRD2, dopamine receptor D2; EGFR, epidermal growth factor receptor; eIF4E, eukaryotic translation initiation factor 4E; EZH2, enhancer of zeste homolog 2; fAUC, fitted area under the curve; FGFR, fibroblast growth factor receptor; HDAC, histone deacetylase; HSP90, heat shock protein 90; KSP, kinesin spindle protein; MDM2, mouse double minute 2 homolog; MEK, mitogen-activated protein kinase kinase; mTOR, mammalian target of rapamycin; PARP, poly(ADP-ribose) polymerase; PD-L1, programmed cell death 1 ligand 1; PLK1, polo-like kinase 1; RAF, rapidly accelerated fibrosarcoma; SMARCA4, SWI/SNF-related, matrix-associated, actin-dependent regulator of chromatin, subfamily A, member 4; SMARCB1, SWI/SNF-related, matrix-associated, actin-dependent regulator of chromatin, subfamily B, member 1; STR, short tandem repeat; XPO1, exportin 1.

* Correspondence to: Pediatric Oncology and Hematology, Children's Hospital, Saarland University, Kirrberger Straße Building 9, Homburg, Saar 66421, Germany.

E-mail address: marc.remke@uks.eu (M. Remke).

<https://doi.org/10.1016/j.phrs.2025.107660>

Received 29 August 2024; Received in revised form 5 February 2025; Accepted 14 February 2025

Available online 16 February 2025

1043-6618/© 2025 The Author(s). Published by Elsevier Ltd. This is an open access article under the CC BY license (<http://creativecommons.org/licenses/by/4.0/>).

ombrabulin hydrochloride (PubChem CID: 6918404)

approach revealed preclinical evidence of tumor type- and subtype-specific therapeutic vulnerabilities in AT/RT cell lines that may inform future *in vivo* and clinical evaluations of novel pharmacological strategies.

1. Introduction

Atypical teratoid/rhabdoid tumor (AT/RT) is a malignant embryonal brain tumor affecting toddlers and infants, and is associated with poor outcome as indicated by a 5-year overall survival of only 34.7 % [1]. AT/RT is molecularly driven by biallelic genetic inactivation of the SWI/SNF-related, matrix-associated, actin-dependent regulator of chromatin, subfamily B, member 1 (*SMARCB1*) in chromosome band 22q11.23 [2–4]. Less commonly, AT/RT feature biallelic inactivation of *SMARCA4* [5]. Other recurrent mutations have not been identified despite comprehensive whole genome sequencing studies [6,7]. However, three AT/RT subtypes with distinct epigenetic and clinical characteristics have been delineated using DNA methylation and expression profiling: AT/RT-TYR, -SHH and -MYC [8]. Further studies revealed a mechanistic interaction between *SMARCB1* inactivation and the epigenetic landscape in AT/RT, and suggested that *SMARCA4*-dependent activation of super enhancers drives AT/RT tumorigenesis [9].

Several early clinical trials investigated targeted therapies based on these epigenetic findings, but none have succeeded in establishing new therapies for AT/RT beyond the current standard of care involving surgical resection, (high-dose) chemotherapy and radiotherapy. Among the pharmacological approaches evaluated for the treatment of AT/RT, different small molecule inhibitors were investigated in clinical trials, including the cyclin-dependent kinase 4/6 (CDK 4/6) inhibitor ribociclib [10], ribociclib combined with the mammalian target of rapamycin (mTOR) inhibitor everolimus [11], the aurora kinase inhibitor alisertib [12], the enhancer of zeste homolog 2 (EZH2) inhibitor tazemetostat [13], the histone deacetylase (HDAC) inhibitor vorinostat combined with the DNA alkylator temozolomide [14] and the gamma secretase inhibitor MK-0752 [15]. However, clinical efficacy remained limited. Trials investigating the poly(ADP-ribose) polymerase (PARP) inhibitor veliparib combined with temozolomide (NCT00946335), the vascular endothelial growth factor receptor (VEGFR) inhibitor AZD2171 (NCT00326664), the farnesyl transferase inhibitor SCH 66336 (NCT00015899), the gamma secretase inhibitor RO4929097 (NCT01088763), the HDAC inhibitor panobinostat (NCT04897880) and the exportin 1 (XPO1) inhibitor selinexor combined with the mouse double minute 2 homolog (MDM2) inhibitor idasanutlin (NCT05952687) were prematurely terminated. Ongoing trials are evaluating the efficacy of the mTOR inhibitor sirolimus (NCT02574728, NCT01331135), the CDK4/6 inhibitor ribociclib, the hedgehog inhibitor sonidegib and the mitogen-activated protein kinase kinase (MEK) inhibitor trametinib (NCT03434262), the CDK4/6 inhibitor palbociclib (NCT03709680), the PARP inhibitor talazoparib combined with the topoisomerase I inhibitor irinotecan (NCT04901702), the dopamine receptor D2 (DRD2) antagonist ONC206 (NCT04541082) and combinatorial treatments involving programmed cell death 1 ligand 1 (PD-L1) antibodies (NCT04416568, NCT05407441 and NCT05286801) as well as chimeric antigen receptor (CAR)-T-cell-based therapy (NCT04483778, NCT03618381, NCT04897321, NCT05835687, NCT04099797 and NCT03638167). An ongoing phase II trial is further investigating the efficacy of tazemetostat (NCT03213665). More recent preclinical studies identified sensitivity of AT/RT to MEK inhibitors [16–20], mouse double minute 2 homolog (MDM2) inhibitors [21], Polo-like kinase 1 (PLK1) inhibitors [22], proteasome inhibitors [23–25] and B-cell lymphoma 2 (BCL2) inhibitors [26].

Here, we employed high-throughput *in vitro* drug screening of AT/RT cell lines combined with large-scale DNA methylation and RNASeq-based expression profiling to characterize novel pharmacological vulnerabilities of AT/RT and its molecular subtypes.

2. Materials and methods

2.1. Cell lines

In total, we investigated thirteen AT/RT, eleven medulloblastoma and eight glioblastoma cell lines. Table S1 provides an overview of all investigated cell lines, their sources, and *in vitro* culture conditions. ATRT-310-FHTC, ATRT-311-FHTC, BT-12SF, BT-16SF and CHLA-266SF showed an adherent growth pattern after the addition of 5 µg/ml (2.5 µg/ml in drug screening) laminin (Cat. No. 354232, Corning, NY, USA) to the cell suspension before plating. Mycoplasma testing was regularly performed using the Venor GeM Advance Kit (Cat. No. 11-7096, Minerva Biolabs, Berlin, Germany) according to the manufacturer's instructions. Cross-contamination was excluded by short tandem repeat (STR) profiling (Genomics & Transcriptomics Laboratory (GTL), Biological And Medical Research Center (BMFZ), Heinrich Heine University Düsseldorf, Düsseldorf, Germany). Seeding density in 384-well plates was optimized for each cell line by performing serial dilutions and subsequent evaluation by estimating confluence or measuring viability plateaus using the CellTiter-Glo assay (G7573, Promega, Madison, WI, USA) (see Section 2.3).

2.2. Drug library and microtiter plate preparation

In vitro drug screening was conducted by printing drug libraries onto 384-well microplates (Cat. No. 3570, Corning, NY, USA) using the D300e Digital Dispenser (Tecan, Männedorf, Switzerland). The Clinical Library Standard (CLS) and the Clinical Library Extended (CLE) drug libraries were obtained from MedChemExpress (Monmouth Junction, NJ, USA). The Tocriscreen Epigenetics Toolbox (EG) and the Tocriscreen Kinase Inhibitor Toolbox (KI) were purchased from Tocris (Minneapolis, MN, USA). Libraries were aliquoted to smaller stock volumes prior to dispensing to avoid repeated thawing. All drugs were printed in a randomized fashion using T8 + dispensehead cassettes (Cat. No. 30097370, Tecan, Männedorf, Switzerland) and afterwards dimethyl sulfoxide (DMSO) volumes were normalized using D4+ dispensehead cassettes (Cat. No. 30097371, Tecan, Männedorf, Switzerland). Multiple plate replicates were prepared in printing cycles, then sealed with parafilm and stored deep frozen at –80 °C until drug screening was conducted. Each plate contained positive controls (Staurosporine, NH 125), at least three DMSO-only wells for normalization and three non-treated wells as negative controls.

2.3. In vitro drug screening

Deep-frozen printed 384-well microtiter plates were thawed at room temperature for approximately 1 h. Simultaneously, cells were harvested and diluted to the previously determined seeding density. Specific information for each cell line is available in Table S1. Each well was filled with 30 µl of cell suspension using the MultiDrop Combi (Thermo Fisher Scientific, Waltham, MA, USA). After plating, cells were incubated at 37 °C and 5 % CO₂ for 72 h. The readout was conducted by measuring viability using the CellTiter-Glo Assay (G7573, Promega, Madison, WI, USA), diluted 1:2 in phosphate-buffered saline. Equal volumes of the reagent were dispensed using the MultiDrop Combi and incubated for 10 min. Then luminescence signal intensity was measured using the Spark plate reader (Tecan, Männedorf, Switzerland) at an integration time of 500 ms.

2.4. RNA sequencing

Total RNA was isolated from cell pellets lysed in TRIZol (Cat. No. 15596018, Thermo Fisher Scientific, Waltham, MA, USA) according to the manufacturer's instructions. After assessing quality and quantifying the RNA using the Agilent RNA 6000 Nano Kit (Cat. No. 5067-1511, Agilent, Santa Clara, CA, USA), the library preparation was performed using the TruSeq RNA Library Preparation Kit v2 (Cat. No. RS-122-2001, Illumina, San Diego, CA, USA). Library concentrations were quantified by means of the Qubit DNA HS Assay-Kit (Cat. No. Q32851, Thermo Fisher Scientific, Waltham, MA, USA) according to the manufacturer's instructions and library quality was assured through the High Sensitivity DNA Kit (Cat. No. 5067-4626, Agilent, Santa Clara, CA, USA). RNA sequencing was performed as described by Forget et al. [27].

2.5. DNA methylation profiling

DNA was isolated from cell pellets using the Bionano Prep Blood and Cell Culture DNA Isolation Kit (Cat. No. 80038, Bionano Genomics, San Diego, CA, USA) and then quantified using the QuantiFluor ONE dsDNA System (Cat. No. E2670, Promega, Madison, WI, USA). DNA methylation profiling was conducted using 850k EPIC bead arrays (Illumina, San Diego, CA, USA) as described by Capper et al. [28]. DNA methylation profiling data were functionally normalized using NOOB background correlation and Dye correction in Partek Genomics Suite (Partek, Chesterfield, MO, USA) for the hierarchical clustering analysis and analyzed with the Brain Tumor Classifier v12.5 (www.moleculareuropathology.org) in parallel. Cell lines were assigned to the methylation class AT/RT and the respective subclasses (AT/RT-SHH, -MYC) based on the calibrated classifier scores provided. Principles of the classifier and DNA methylation classes/subclasses have been published by Capper et al. [28]. DNA copy number profiles were additionally derived from the array data using the "conumee" package for R (<http://bioconductor.org/packages/conumee>).

2.6. Data analyses

Drug activity (i.e. dose-dependent reduction of tumor cell growth) was measured using fitted area under the curve (fAUC) data, relative IC₅₀ (i.e. the drug concentration that achieves half-maximal growth reduction in nM), and bottom levels (i.e. maximum growth inhibition achieved in %), all of which were determined in Prism 7 (GraphPad, San Diego, CA, USA). Specifically, we use a five-parametric logistic fitting employing constraints of the top level, the bottom level and the IC₅₀ range. The fAUC was calculated by normalizing to a flat dose-response curve which indicated no effect (i.e. growth inhibition) up to a concentration of 25.000 nM. An fAUC of 0 thus indicates no effect and an fAUC of 1 indicates maximum growth inhibition at lowest concentrations. A negative fAUC may occur if a drug caused growth acceleratory effects. For the analyses in this study, negative fAUC values were constrained to zero. To visualize the data dose-response curves and volcano/scatter plots were rendered in Prism 7. Significance in drug screening data was assessed using the Mann-Whitney-U test on fAUC data of different sets of cell lines. P-values < 0.05 were considered significant. Hierarchical clustering analyses and corresponding heatmaps were generated in RStudio (Posit, Boston, MA, USA) using the complexheatmap and factoextra packages. Spearman correlation was used for distance calculation of the drug screening data, if not stated otherwise, and Pearson correlation for the DNA methylation profiling and RNASeq-based expression profiling data. Average linkage was used for agglomeration in all analyses.

3. Results

3.1. AT/RT cell lines exhibit a specific sensitivity to MEK and MDM2 inhibitors

To identify drugs with selective activity in AT/RT cell lines, we compared drug screening data from 13 AT/RT cell lines to a reference cohort consisting of eleven medulloblastoma cell lines and eight glioblastoma cell lines. For this purpose, data obtained with all four drug libraries were pooled, amounting to the *in vitro* evaluation of 735–772 distinct drugs. We calculated fold changes and p-values, and filtered the data for a mean fitted area under the curve (fAUC) of 0.2 in AT/RT cell lines to eliminate drugs with low activity. A volcano plot was generated that revealed multiple AT/RT-selective inhibitors, specifically multiple mitogen-activated protein kinase kinase (MEK) (n = 11) and mouse double minute 2 homolog (MDM2) (n = 4) inhibitors (Fig. 1A). Drug class-wise analyses (Fig. S1A) confirmed the preferential inhibition of AT/RT cell lines by MEK and MDM2 inhibitors with mean fAUC scores of 0.289 (0.101–0.502) and 0.298 (0.187–0.393) and IC₅₀ values of 1311 nM (430–2878 nM) and 2514 nM (1500–4825 nM) in AT/RT cell lines compared to mean fAUC scores of 0.120 (0.025–0.482) and 0.129 (0.028–0.391) and IC₅₀ values of 4782 nM (256–8863 nM) and 5653 nM (1042–13164 nM) in the control cohort of glioblastoma and medulloblastoma cell lines, which corresponds to fold changes of 2.41 and 2.31 and p-values of 0.00007 and 0.0024, respectively. A detailed collection of activity parameters of drugs with significantly increased activity in AT/RT cell lines is provided in Table S3. The individual dose-response curves of the most active drugs revealed an early onset of effect (lower IC₅₀ values) for the MEK inhibitor GDC-0623 (Fig. 1B) and the MDM2 inhibitor idasanutlin (Fig. 1C), but later onset of effect (higher IC₅₀ values) for the fibroblast growth factor receptor (FGFR) inhibitor zoligrafatinib (Fig. 1D) and the epidermal growth factor receptor (EGFR) inhibitor poziotinib (Fig. 1E). Consistently, the ratio of drug activity and fold change was higher for MEK and MDM2 inhibitors than for FGFR and EGFR inhibitors (Fig. S1B). With respect to EGFR inhibition, further analyses indicated that three AT/RT cell lines (BT-16SF, CHLA-266SF and VU397) were exceptionally sensitive (Fig. S1C). Moreover, ATRT13808 displayed rapidly accelerated fibrosarcoma (RAF) inhibitor-sensitivity (Fig. S1D). Thus, our comparative analysis of the most common malignant brain tumors in infants, children, and adults revealed sensitivity of AT/RT to targeted therapeutic approaches including MEK and MDM2 inhibition.

3.2. DNA methylation and RNASeq-based gene expression profiling reveal that heterogenous drug response profiles are linked to molecular subtypes of AT/RT

We analyzed for heterogenous drug responses using hierarchical clustering analysis, which derived two main clusters among the AT/RT cell lines (Fig. 2A). We complemented the drug screening data with additional DNA methylation and RNASeq-based gene expression data (paired-end sequencing, at least 60x coverage) from the corresponding cell lines and performed hierarchical clustering analysis with these layers of data. Notably, the drug screening data-based subgroups were corroborated in both datasets (Fig. 2B and C). Performing methylation class prediction using the Brain Tumor Classifier (v12.5) revealed that these subgroups corresponded to the biological subtypes of AT/RT, comprising six AT/RT-SHH cell lines (ATRT-310-FHTC, ATRT-311-FHTC, CHLA-02, CHLA-04, CHLA-05 and HHU-ATRT-01) and seven AT/RT-MYC cell lines (ATRT13808, BT-12SF, BT-16SF, CHLA-06, CHLA-266SF, JC-ATRT and VU397) (Table S2). AT/RT-TYR cell lines were not present among the investigated AT/RT models, as there are currently none known for this particular subtype. In summary, heterogenous drug response profiles were attributed to molecular subtypes of AT/RT.

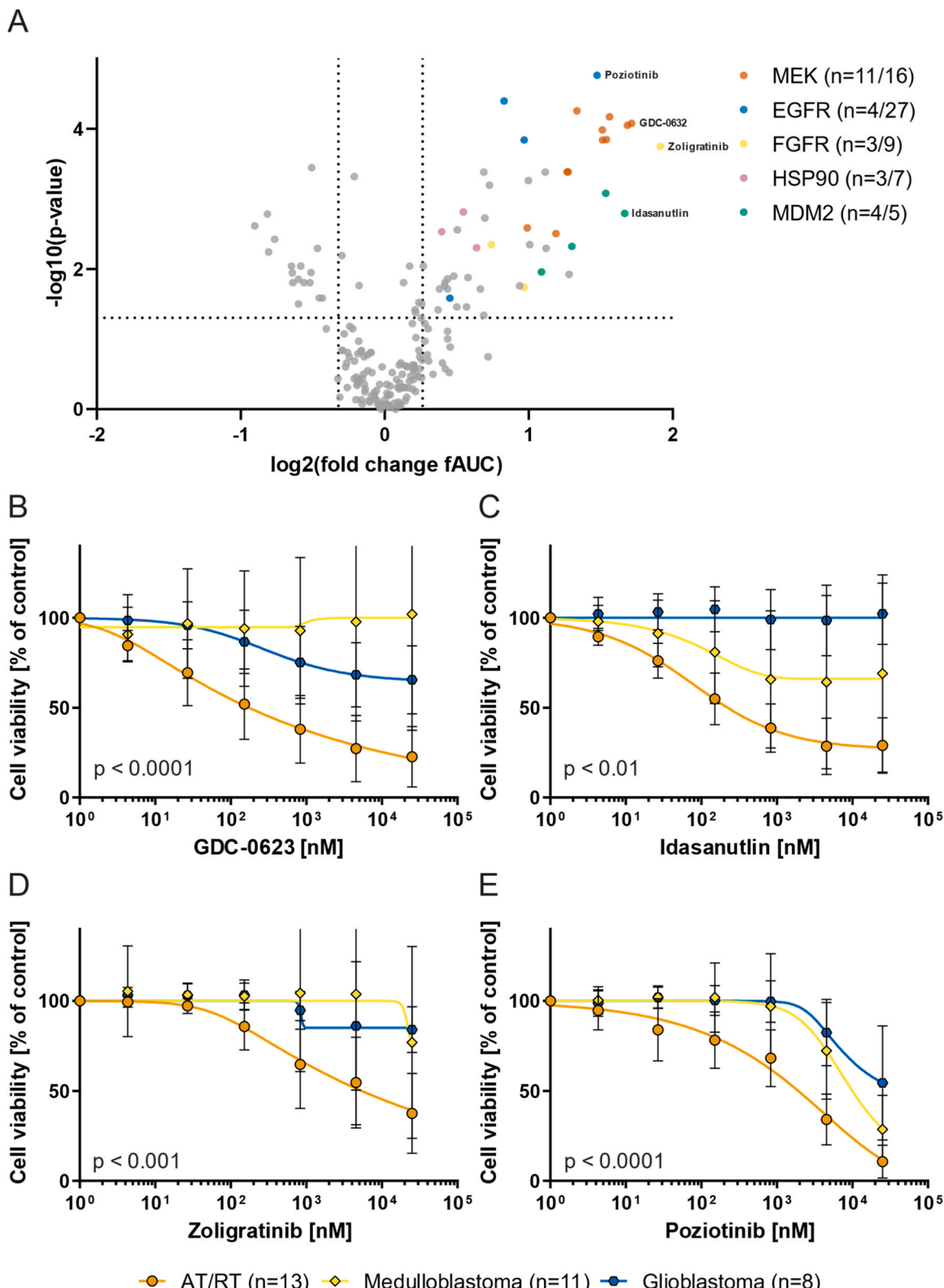


Fig. 1. *In vitro* drug screening reveals specific activity of MEK and MDM2 inhibitors in AT/RT cell lines. Drug screening results obtained by comparing drug responses of AT/RT cell lines ($n = 13$) against drug responses of a control cohort of medulloblastoma cell lines ($n = 11$) and glioblastoma cell lines ($n = 8$). (A) Volcano plot based on p-value (Mann-Whitney-U test) and fold change of fitted area under the curve (fAUC) data depicting drugs with significantly increased activity in AT/RT cell lines compared to medulloblastoma and glioblastoma cell lines. Drug classes with multiple occurrences are highlighted and the top candidate drugs are labeled. The dotted lines indicate a fold change of 0.8 or 1.2 or a p-value of 0.05. (B-E) Cumulative dose-response curves of AT/RT, medulloblastoma and glioblastoma cell lines showing increased activity in AT/RT cell lines with early onset of effect of the mitogen-activated protein kinase kinase (MEK) inhibitor GDC-0623 (B) and the mouse double minute 2 homolog (MDM2) inhibitor idasanutlin (C), compared to lower activity with later onset of effect of the fibroblast growth factor receptor (FGFR) inhibitor zoligatinib (D) and the epidermal growth factor receptor (EGFR) inhibitor poziotinib (E). P-values below the dose-response curves rely on a Mann-Whitney-U test of fAUC data from AT/RT cell lines vs. medulloblastoma and glioblastoma cell lines. Error bars indicate SD.

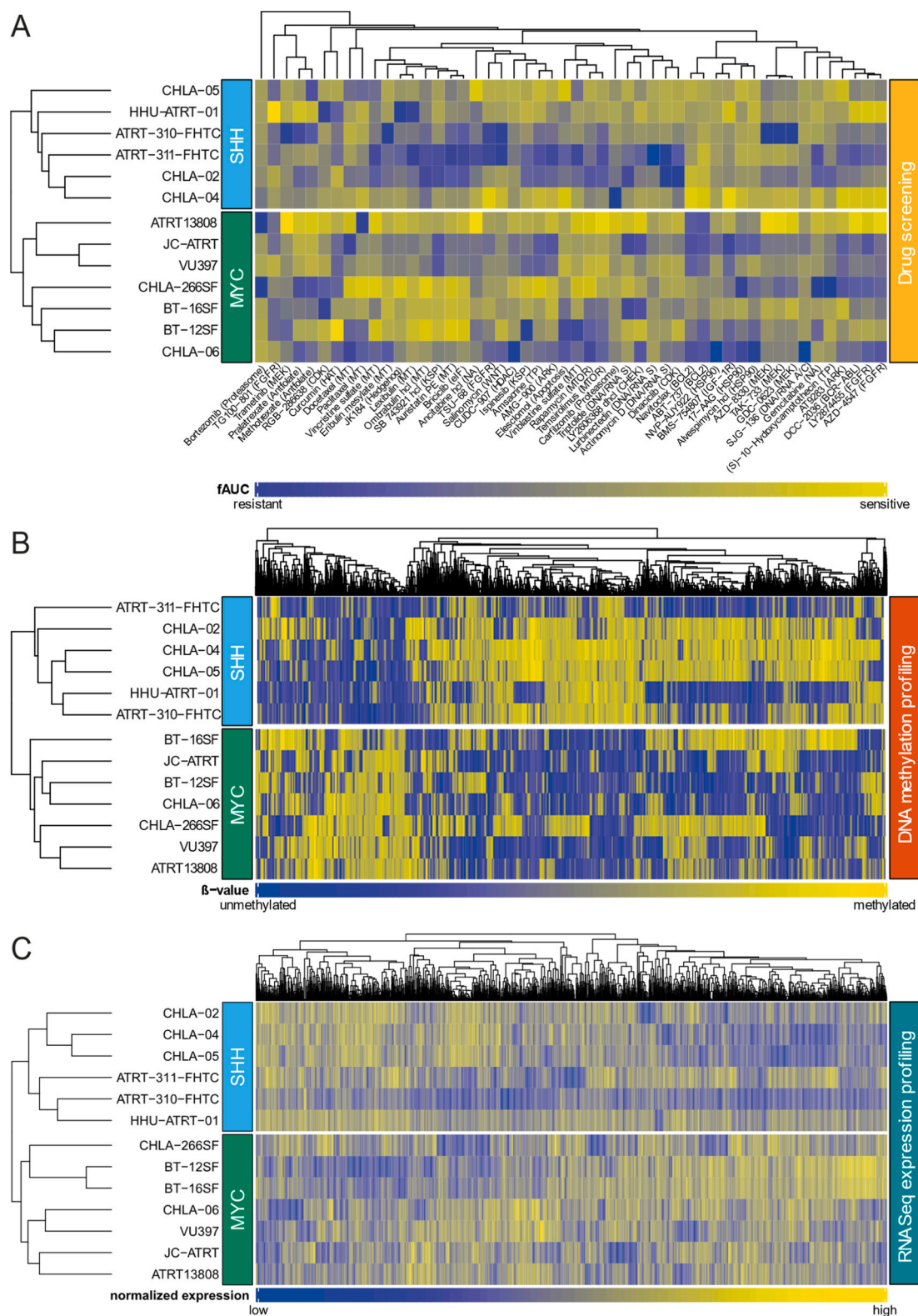


Fig. 2. DNA methylation profiling and RNASeq-based expression profiling link heterogeneous drug response patterns to molecular subtypes of AT/RT. Hierarchical clustering analyses of fitted area under the curve (fAUC) data from drug screening (A), beta values from DNA methylation profiling (B) and normalized expression from RNASeq-based expression profiling (C). (A) The drug screening data were filtered to exceed an fAUC of 0.1 in at least one AT/RT cell line to remove any drugs with no activity. Thus, the top 50 drugs according to standard deviation were used for clustering. Two clusters with distinct drug sensitivity profiles emerged. (B) Beta values from DNA methylation profiling data using 850k EPIC bead arrays. The top 5.000 sites according to standard deviation are shown. (C) RNASeq-based expression profiling data including the top 10 % of differentially regulated genes based on standard deviation. Both DNA methylation profiling and RNASeq-based expression profiling corroborated the drug screening-based subgrouping of the AT/RT cell lines. All clusters were associated with the molecular subtypes of AT/RT by means of classification using the Brain Tumor Classifier v12.5 (<http://www.molecularneuropathology.org/mnp>), see Table S2.

3.3. Pharmacogenomic approach reveals subtype-specific vulnerabilities in AT/RT

For the identification of subtype-specific inhibitors, we compared both subtypes defined previously using (epi-)genomic data and generated a volcano plot (Fig. 3A), calculating fold changes and p-values from the comparison of AT/RT-SHH vs. -MYC. The AT/RT-SHH subtype cell lines showed an enrichment for multiple B-cell lymphoma 2 (BCL2) ($n = 3$) and heat shock protein 90 (HSP90) ($n = 4$) inhibitors. The mean fold changes were 4.49 (p-value 0.001) and 1.47 (p-value 0.018) for the top candidates, ABT-737 (BCL2 inhibitor) and 17-AAG (HSP90 inhibitor), respectively, which corresponded to mean fAUC values of 0.370 and 0.629 and mean IC₅₀ values of 510 nM and 36 nM in AT/RT-SHH cell lines compared to mean fAUC values of 0.083 and 0.428 as well as mean IC₅₀ values of 6127 nM and 506 nM in AT/RT-MYC cell lines, respectively. The corresponding dose-response curves are depicted in Fig. 3B and C, and a collection of activity parameters of drugs with significantly increased activity in AT/RT-SHH cell lines is provided in Table S4. In addition, Notch inhibitors ($n = 3$) exhibited low activity in AT/RT-SHH cell lines, while we observed no activity in AT/RT-MYC cell lines, as indicated by a high drug class-wise fold change of 3.41 (Fig. S2A), but low activity in the corresponding dose-response curve of the top candidate MK-0752 (Fig. S2C). Consequently, Notch inhibitors show low ratios of drug activity vs fold change (Fig. S2E). Regarding drugs with selective activity in the AT/RT-MYC subtype, we identified a subset of microtubule inhibitors, along with the eukaryotic translation initiation factor 4E (eIF4E) inhibitor briciclib as being preferentially active. The dose-response curves of the top candidates ombrabulin hydrochloride and briciclib are depicted in Fig. 3D and E. Moreover, the dose-response curve of pelitinib, an EGFR inhibitor, displays narrow but significant (p-value 0.018) selectivity for AT/RT-MYC cell lines (Fig. S2D). However, a drug class-wise analysis indicated no significant enrichment of drug classes in AT/RT-MYC (Fig. S2B). Detailed activity parameters of drugs with significantly increased activity in AT/RT-MYC cell lines are provided in Table S5. Notably, more detailed analyses indicated that AT/RT-MYC cell lines separate into four cell lines with increased sensitivity to microtubule inhibitors (Microtubule-sensitive (MT-s) cohort), and three cell lines exhibiting sensitivity profiles similar to those of AT/RT-SHH cell lines (Microtubule-resistant (MT-r) cohort) (Fig. 4A). We thus compared drug response profiles in cell lines from the MT-s cohort vs. all other AT/RT cell lines. Thereby, we detected multiple drugs related to microtubule functioning to be significantly enriched, like kinesin spindle protein (KSP) inhibitors, and found further enrichment of the microtubule inhibitor ombrabulin hydrochloride (Fig. 4B) and the eIF4E inhibitor briciclib (Fig. 4C). Table S6 summarizes detailed drug activity parameters of the MT-s cohort of AT/RT-MYC cell lines. Notably, we found an activation of eIF4E signaling using the data from RNASeq-based expression profiling comparing the MT-s cohort vs. other AT/RT cell lines (data not shown). Taken together, our pharmacogenomic approach detected subtype-specific targeted therapies for the treatment of AT/RT-SHH and -MYC subtypes.

4. Discussion and conclusion

Our pharmacogenomic study of AT/RT cell lines combines comprehensive *in vitro* drug screening of clinically available and late-stage developmental drugs with large-scale DNA methylation and RNASeq-based gene expression profiling, providing evidence for novel subtype-specific targeted therapeutic approaches.

The clinical aggressiveness of AT/RT is evident, as overall and progression-free survival rates remain poor despite intensive multimodal treatment. In addition, aggressive therapy of AT/RT often causes lasting sequelae in the rare long-term survivors, specifically because of the early disease onset, mostly during infancy. While these facts highlight the urgent need for targeted therapies to be developed for the effective and safe treatment of AT/RT, such treatments are not yet

available even though tremendous progress has been made toward the understanding of AT/RT's biology. Notably, our approach initially compared drug sensitivity profiles of AT/RT models with other highly aggressive brain tumor models derived from glioblastomas and medulloblastomas. Comparative analysis of high-resolution dose-response data with six to eleven dilution steps comprised 768 drugs from four different libraries, most of which contained drugs that are clinically available, including conventional chemotherapeutic agents [29,30] and established antiproliferative drugs [31,32], or currently undergoing the late stages of drug development. The results indicated preferential therapeutic activity of multiple MEK and MDM2 inhibitors, further promoting the efficacy of these drug classes for the treatment of AT/RT, in line with previous reports [16–21].

In addition, we provide preclinical evidence of molecular subtype-specific drug activities by the incorporation of DNA methylation profiling and RNASeq-based gene expression data, which allowed us to separate our cohort of 13 AT/RT cell lines into six AT/RT-SHH cell lines and seven AT/RT-MYC cell lines. Thus, heterogenous drug response profiles resolved into subtype-specific response patterns. We found highly specific class-wide activity of BCL2 inhibitors in AT/RT-SHH cell lines, with ABT-737 and ABT-199 (venetoclax) being most selective. Sensitivity of AT/RT-SHH cell lines to venetoclax was previously described by Paassen et al. [26]. Moreover, preferential and potent inhibition of AT/RT-SHH cell lines at low-nanomolar range was observed for HSP90 inhibitors, most prominently 17-AAG (tanespimycin). A subset of the AT/RT-MYC cell lines showed increased sensitivity to microtubule inhibitors, KSP inhibitors and the eIF4E inhibitor briciclib. Vincristine, one of the microtubule inhibitors with preferential activity in AT/RT-MYC, is frequently administered to AT/RT patients during adjuvant chemotherapy, which raises the question of whether these patients exhibit prolonged survival, especially when stratified for the AT/RT-MYC subtype. Consequently, it may be of interest to explore the efficacy-safety profile of drugs with comparable efficacy to vincristine, such as ombrabulin hydrochloride or lexibulin, and potentially optimize treatment protocols by increasing dosages of microtubule inhibitors, if possible, and omitting the application of other drugs in order to prevent unnecessary additional toxicity. Notably, ombrabulin hydrochloride and lexibulin did not exhibit such a distinct response pattern as other microtubule-targeted drugs in AT/RT-MYC cell lines segregated according to the general response of this drug class (Tables S5 and S6). This indicates that these two inhibitors may constitute highly attractive drug candidates for the majority of AT/RT-MYC tumors. A potential approach to further increase the efficacy of the identified (subtype-specific) drugs lies in a combination treatment using two or more drugs, which could promote synergistic effects, and thus, reduce the required dosages for each drug. Since *in vitro* models of AT/RT-TYR are not yet available, we unfortunately cannot provide any results concerning the chemosensitivity of this AT/RT subtype.

Pharmacokinetic properties like oral bioavailability and brain permeability in the setting of an intact blood brain barrier constitute a critical aspect for the efficacy of drugs used in patients with brain tumors. MEK inhibitors are increasingly used for the treatment of low-grade gliomas, showing superior response rates over conventional chemotherapy [33–35], and the MDM2 inhibitor idasanutlin has been proven to sufficiently cross the blood brain barrier in previous studies [36]. Thus, the pan-AT/RT candidate drugs identified in our study fulfill these pharmacokinetic requirements. However, we believe future therapy of AT/RT should focus on subtype-specific approaches, as they take certain biological traits of AT/RT tumorigenesis into account. Furthermore, subtype determination using DNA methylation profiling-based classification has become part of routine clinical diagnostic workup. Regarding the subtype-specific drugs, ABT-737 lacks oral bioavailability, which is why navitoclax, an orally bioavailable derivative of ABT-737, was developed [37,38]. ABT-199 (venetoclax) comprises another derivative of ABT-737 that is orally bioavailable and brain permeable [39]. In our study, both navitoclax and ABT-199 deliver

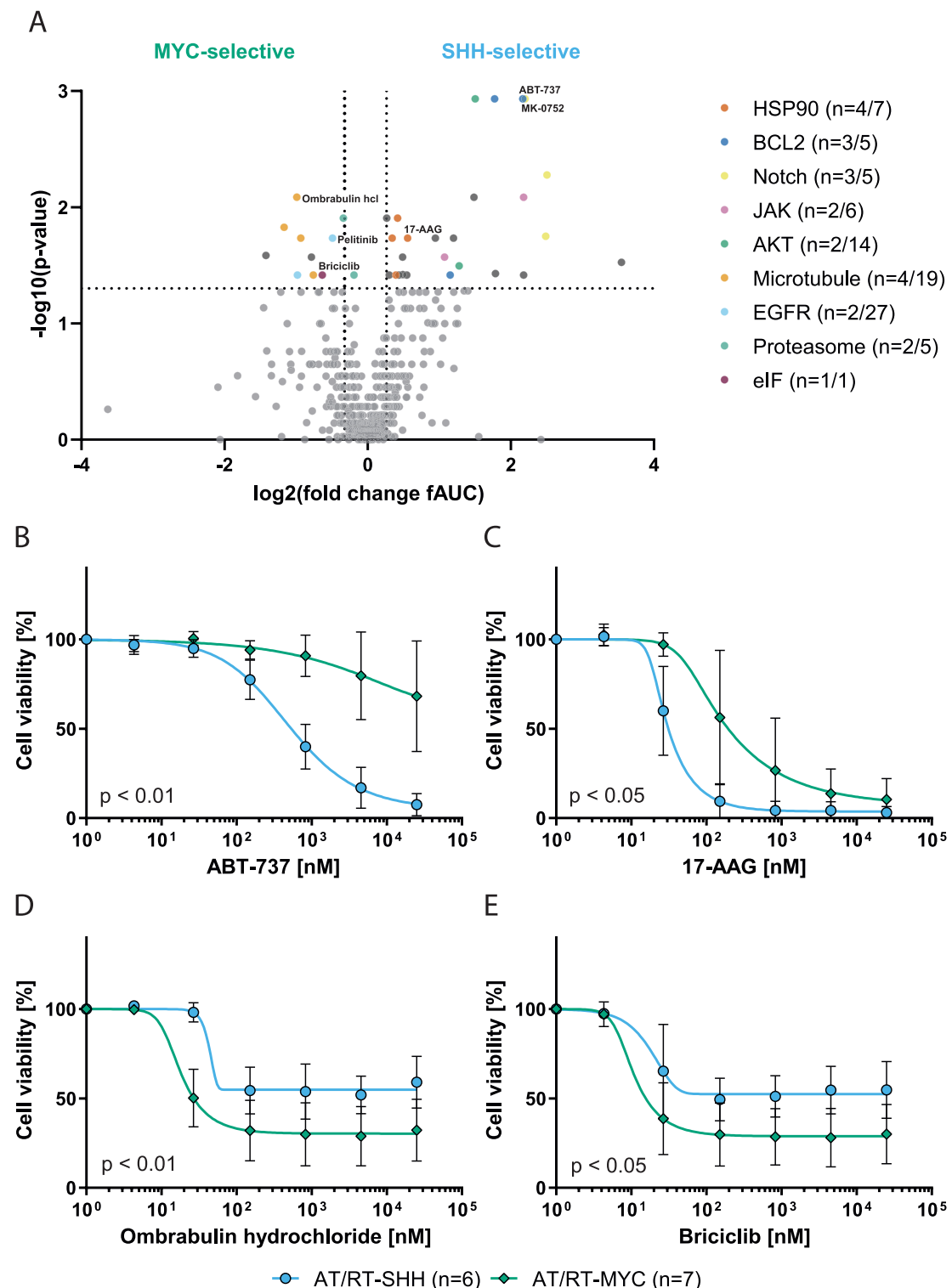


Fig. 3. Pharmacogenomic approach reveals subtype-specific drug vulnerabilities in AT/RT. Analysis of heterogeneity in AT/RT drug screening data by subtype stratification. (A) A volcano plot based on p-value (Mann-Whitney-U test) and fold change revealed numerous drugs with selective activity in AT/RT-MYC cell lines (left side of the plot) and AT/RT-SHH cell lines (right side of the plot). Drug classes that appeared multiple times were highlighted, and the top drugs of each drug class were labeled. The dotted lines indicate a fold change of 0.8 or 1.2 or a p-value of 0.05. (B-C) AT/RT-SHH cell lines showed increased sensitivity to B-cell lymphoma 2 (BCL2) and heat shock protein 90 (HSP90) inhibitors, most prominently the BCL2 inhibitor ABT-737 (B) and the HSP90 inhibitor 17-AAG (C), as visualized in the corresponding dose-response curves. (D-E) AT/RT-MYC cell lines showed increased sensitivity to microtubule inhibitors, most prominently ombrabulin hydrochloride (D), and the eukaryotic translation initiation factor 4E (eIF4E) inhibitor briciclib (E), as visualized in the corresponding dose-response curves. P-values below the dose-response curves rely on a Mann-Whitney-U test of fAUC data from AT/RT-SHH cell lines vs. AT/RT-MYC cell lines. Error bars indicate SD.

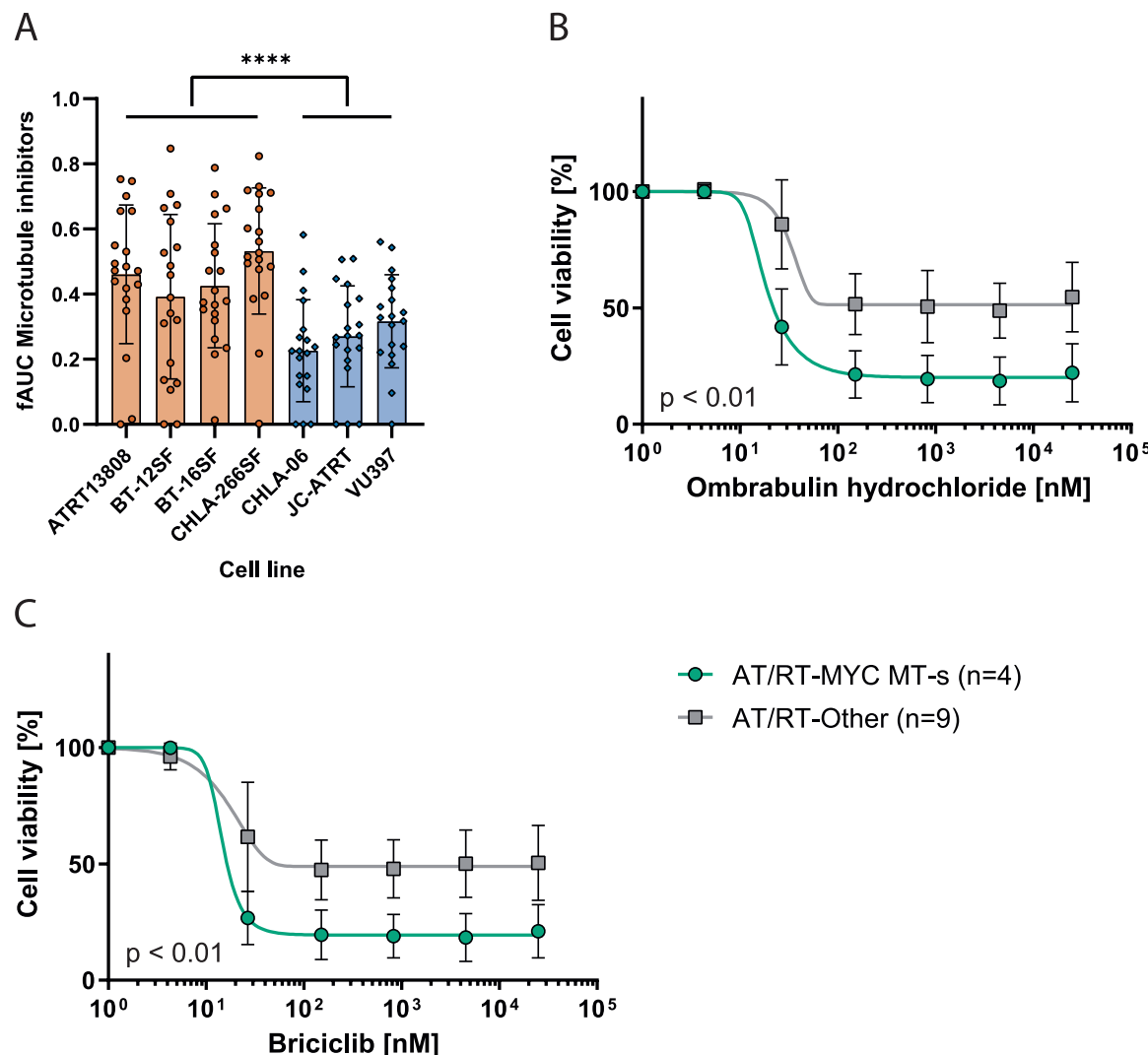


Fig. 4. AT/RT-MYC cell lines partially respond to microtubule inhibitors, kinesin spindle protein (KSP) inhibitors and the eIF4E inhibitor briciclib. Analysis of distinct heterogenous drug responses of AT/RT-MYC cell lines. (A) A bar plot displaying fitted area under the curve (fAUC) data of all microtubule inhibitors contained in the investigated drug libraries indicated that four out of seven AT/RT-MYC cell lines harbor an increased sensitivity to microtubule inhibitors (MT-sensitive (s) and MT-resistant (r) cohorts). (B) The dose-response curve of the top candidate, ombrabulin hydrochloride, visualizing the increased activity in the MT-s cohort of AT/RT-MYC while the other AT/RT-MYC cell lines align with the AT/RT-SHH cell lines and were thus summarized as AT/RT-Other. (C) The eukaryotic translation initiation factor 4E (eIF4E) inhibitor briciclib showed a comparable dose-response profile with increased activity in the MT-s cohort of AT/RT-MYC. P-values below the dose-response curves rely on a Mann-Whitney-U test of fAUC data from AT/RT-MYC MT-s cell lines vs. other AT/RT cell lines. Error bars indicate SD.

selectivity for AT/RT-SHH, but lower activity/fold change compared to ABT-737 (Table S4). 17-AAG, one of the HSP90 inhibitors that was discovered to harbor AT/RT-SHH-selective properties in our study, demonstrated some limited brain permeability, but poor oral bioavailability, and also caused dose-limiting hepatotoxicity [40,41]. Ganetespib and NVP-AUY922, both of which are second-generation HSP90 inhibitors, delivered lower fold changes compared to 17-AAG, but still demonstrate selectivity for AT/RT-SHH (Table S4). Second-generation HSP90 inhibitors lack hepatotoxic effects [42], which may justify prioritizing these over first-generation HSP90 inhibitors, especially in light of prolonged treatment duration, although they also require parenteral administration [43,44] and robust data pertaining to their brain permeability is still lacking. Regarding the proposed candidates for the treatment of AT/RT-MYC, both ombrabulin hydrochloride and lexibulin performed equally in drug screening. However, among these two candidate drugs, lexibulin has documented oral bioavailability, making it more attractive for further clinical evaluation [45,46].

Taken together, our pharmacogenomic *in vitro* study substantiates

known targets in AT/RT and reveals experimental evidence for therapeutic vulnerabilities for this high-risk brain tumor in infants in a subtype-specific manner. Further studies are necessary to functionally validate the identified drug responses and characterize their underlying mechanisms. Moreover, the analysis of a larger cohort of AT/RT samples may allow to gain more profound insights into the drivers of (subtype-dependent) drug sensitivities to potentially establish reliable biomarkers. Irrespective of further *in vitro* studies, the identified targets and drugs are promising candidates for further preclinical *in vivo* evaluation and eventually clinical translation into novel therapeutic strategies that might hopefully lead to improved outcomes of AT/RT patients.

Funding

This study was funded by the Deutsche Krebshilfe (German Cancer Aid, Grant No. 589 111537, awarded to Guido Reifenberger and Marc Remke), the Elterninitiative Kinderkrebsklinik e.V. (awarded to Marc Remke and Jasmin Bartl), the Gert und Susanna Mayer Stiftung

(awarded to Marc Remke), the Research Commission of the Medical Faculty, Heinrich Heine University Düsseldorf (awarded to Marc Remke and Nan Qin), and the Deutsche Forschungsgemeinschaft (German Research Foundation, Grant No. RE 2857/2-1 awarded to Marc Remke, Grant No. RE 938/4-1 awarded to Guido Reifenberger and Grant No. KFO 337 awarded to Marc Remke). Marc Remke received funding from the Saarländische Krebsliga. David Pauck received an MD scholarship from the Kind-Philipp-Stiftung für pädiatrisch-onkologische Forschung.

CRediT authorship contribution statement

Dominik Schöndorf: Writing – review & editing, Resources, Project administration. **Frauke-Dorothee Meyer:** Investigation. **Johanna Theruvath:** Investigation. **David Pauck:** Writing – review & editing, Writing – original draft, Visualization, Project administration, Methodology, Investigation, Funding acquisition, Formal analysis, Data curation, Conceptualization. **Siddhartha Mitra:** Writing – review & editing, Resources, Project administration. **Martin Hasselblatt:** Writing – review & editing, Resources, Project administration. **Michael C. Frühwald:** Writing – review & editing, Resources, Project administration. **Guido Reifenberger:** Writing – review & editing, Writing – original draft, Supervision, Resources, Project administration, Funding acquisition, Conceptualization. **Daniel Picard:** Visualization, Formal analysis, Data curation. **Mara Maué:** Investigation. **Kübra Taban:** Investigation. **Viktoria Marquardt:** Methodology, Investigation. **Lena Blümel:** Investigation, Funding acquisition. **Jasmin Bartl:** Supervision, Project administration, Funding acquisition, Data curation. **Nan Qin:** Supervision, Project administration, Funding acquisition, Data curation. **Nadezhda Kubon:** Investigation.

Declaration of Competing Interest

The authors declare that they have no known competing financial interests or personal relationships that could have appeared to influence the work reported in this paper.

Acknowledgements

The authors would like to thank Anna Kaufhold and Sarah Göbbels for practical instructions and technical support of this project. Furthermore, we thank the Seattle Children's Research Institute for providing ATRT-310-FHTC and ATRT-311-FHTC cell lines and the Japanese Collection of Research Bioresources Cell Bank (JCRB) for providing AM-38 and YH-13 cell lines. The graphical abstract was created in BioRender (<https://Biorender.com/e33k092>).

Appendix A. Supporting information

Supplementary data associated with this article can be found in the online version at [doi:10.1016/j.phrs.2025.107660](https://doi.org/10.1016/j.phrs.2025.107660).

Data availability

Data of the DNA methylation profiling and the RNASeq-based expression profiling have been deposited in the GEO repository (<https://www.ncbi.nlm.nih.gov/geo/>) under the accession numbers GSE282878 and GSE282972, respectively. Drug screening data will be made available upon reasonable request.

References

- [1] M.C. Frühwald, M. Hasselblatt, K. Nemes, S. Bens, M. Steinbügl, P.D. Johann, K. Kerl, P. Hauser, E. Quiroga, P. Solano-Paez, V. Biassoni, M.J. Gil-da-Costa, M. Perek-Polnik, M. van de Wetering, D. Sumerauer, J. Pears, N. Stabell, S. Holm, H. Hengartner, N.U. Gerber, M. Grotzer, J. Boos, M. Ebinger, S. Tippelt, W. Paulus, R. Furtwängler, P. Hernáiz-Driever, H. Reinhard, S. Rutkowski, P.G. Schlegel, I. Schmid, R.D. Kortmann, B. Timmermann, M. Warmuth-Metz, U. Kordes, J. Gerss, K. Nysom, R. Schneppenheim, R. Siebert, M. Kool, N. Graf, Age and DNA methylation subgroup as potential independent risk factors for treatment stratification in children with atypical teratoid/rhabdoid tumors, *Neuro Oncol.* 22 (7) (2020) 1006–1017.
- [2] J.A. Biegel, Molecular genetics of atypical teratoid/rhabdoid tumor, *Neurosurg. Focus* 20 (1) (2006) E11.
- [3] D.N. Louis, A. Perry, G. Reifenberger, A. von Deimling, D. Figarella-Branger, W. K. Cavenee, H. Ohgaki, O.D. Wiestler, P. Kleihues, D.W. Ellison, The 2016 world health organization classification of tumors of the central nervous system: a summary, *Acta Neuropathol.* 131 (6) (2016) 803–820.
- [4] A.R. Judkins, J. Mauger, A. Ht, L.B. Rorke, J.A. Biegel, Immunohistochemical analysis of hSNF5/INI1 in pediatric CNS neoplasms, *Am. J. Surg. Pathol.* 28 (5) (2004) 644–650.
- [5] M. Hasselblatt, S. Gesk, F. Oyen, S. Rossi, E. Viscardi, F. Giangaspero, C. Giannini, A.R. Judkins, M.C. Frühwald, T. Obser, R. Schneppenheim, R. Siebert, W. Paulus, Nonsense mutation and inactivation of SMARCA4 (BRG1) in an atypical teratoid/rhabdoid tumor showing retained SMARCB1 (INI1) expression, *Am. J. Surg. Pathol.* 35 (6) (2011) 933–935.
- [6] M. Hasselblatt, S. Isken, A. Linge, K. Eikmeier, A. Jeibmann, F. Oyen, I. Nagel, J. Richter, K. Bartelheim, U. Kordes, R. Schneppenheim, M. Frühwald, R. Siebert, W. Paulus, High-resolution genomic analysis suggests the absence of recurrent genomic alterations other than SMARCB1 aberrations in atypical teratoid/rhabdoid tumors, *Genes Chromosomes Cancer* 52 (2) (2013) 185–190.
- [7] J.I. Hoell, M. Gombert, C. Bartenhagen, S. Ginzel, P. Husemann, J. Felsberg, G. Reifenberger, A. Eggert, M. Dugas, S. Schonberger, A. Borkhardt, U. Fischer, Whole-genome paired-end analysis confirms remarkable genomic stability of atypical teratoid/rhabdoid tumors, *Genes Chromosomes Cancer* 52 (10) (2013) 983–985.
- [8] P.D. Johann, S. Erkek, M. Zapatka, K. Kerl, I. Buchhalter, V. Hovestadt, D.T. Jones, D. Sturm, C. Hermann, M. Segura Wang, A. Korshunov, M. Rhyzova, S. Grobner, S. Brabetz, L. Chavez, S. Bens, S. Groschel, F. Kratochwil, A. Wittmann, L. Sieber, C. Georg, S. Wolf, K. Beck, F. Oyen, D. Capper, P. van Sluis, R. Volckmann, J. Koster, R. Versteeg, A. von Deimling, T. Milde, O. Witt, A.E. Kulozik, M. Ebinger, T. Shalaby, M. Grotzer, D. Sumerauer, J. Zamecník, J. Mora, N. Jabado, M. D. Taylor, A. Huang, E. Aronica, A. Bertoni, B. Radlwimmer, T. Pietsch, U. Schuller, R. Schneppenheim, P.A. Northcott, J.O. Korbel, R. Siebert, M.C. Frühwald, P. Lichter, R. Eils, A. Gajjar, M. Hasselblatt, S.M. Pfister, M. Kool, Atypical teratoid/rhabdoid tumors are comprised of three epigenetic subgroups with distinct enhancer landscapes, *Cancer Cell* 29 (3) (2016) 379–393.
- [9] S. Erkek, P.D. Johann, M.A. Finetti, Y. Drosos, H.C. Chou, M. Zapatka, D. Sturm, D. T.W. Jones, A. Korshunov, M. Rhyzova, S. Wolf, J.P. Mallm, K. Beck, O. Witt, A. E. Kulozik, M.C. Frühwald, P.A. Northcott, J.O. Korbel, P. Lichter, R. Eils, A. Gajjar, C.W.M. Roberts, D. Williamson, M. Hasselblatt, L. Chavez, S.M. Pfister, M. Kool, Comprehensive analysis of chromatin states in atypical teratoid/rhabdoid tumor identifies diverging roles for SWI/SNF and polycomb in gene regulation, *Cancer Cell* 35 (1) (2019) 95–110.e8.
- [10] B. Georger, F. Bourdeaut, S.G. DuBois, M. Fischer, J.I. Geller, N.G. Gottardo, A. Marabelle, A.D.J. Pearson, S. Modak, T. Cash, G.W. Robinson, M. Motta, A. Matano, S.G. Bhanali, J.R. Dobson, S. Parasuraman, S.N. Chi, A Phase I study of the CDK4/6 inhibitor ribociclib (LEE011) in pediatric patients with malignant rhabdoid tumors, neuroblastoma, and other solid tumors, *Clin. Cancer Res.* 23 (10) (2017) 2433–2441.
- [11] M.D. DeWire, C. Fuller, O. Campagne, T. Lin, H. Pan, T. Young Poussaint, P. A. Baxter, E.I. Hwang, A. Bukowinski, K. Dorris, L. Hoffman, A.J. Waanders, M. A. Karajannis, C.F. Stewart, A. Onar-Thomas, M. Fouladi, I.J. Dunkel, A. Phase, I and surgical study of ribociclib and everolimus in children with recurrent or refractory malignant brain tumors: a pediatric brain tumor consortium study, *Clin. Cancer Res.* 27 (9) (2021) 2442–2451.
- [12] S.A. Upadhyaya, O. Campagne, C.A. Billups, B.A. Orr, A. Onar-Thomas, R. G. Tatevossian, R. Mostafavi, J.R. Myers, A. Vinitsky, D.C. Moreira, H.B. Lindsay, L. Kilburn, P. Baxter, A. Smith, J.R. Crawford, S. Partap, A.E. Bendel, D.G. Aguilera, K.E. Nichols, E. Rampersaud, D.W. Ellison, P. Klimo, Z. Patay, G.W. Robinson, A. Broniscer, C.F. Stewart, C. Wetmore, A. Gajjar, Phase II study of alisertib as a single agent for treating recurrent or progressive atypical teratoid/rhabdoid tumor, *Neuro Oncol.* (2022).
- [13] American Association for Cancer Research Rare Tumors in Kids May Respond to Tazemetostat, *Cancer Discov.* 8(1) (2018) Of5.
- [14] T.R. Hummel, L. Wagner, C. Ahern, M. Fouladi, J.M. Reid, R.M. McGovern, M. M. Ames, R.J. Gilbertson, T. Horton, A.M. Ingle, B. Weigel, S.M. Blaney, A pediatric phase 1 trial of vorinostat and temozolamide in relapsed or refractory primary brain or spinal cord tumors: a Children's Oncology Group phase 1 consortium study, *Pediatr. Blood Cancer* 60 (9) (2013) 1452–1457.
- [15] M. Fouladi, C.F. Stewart, J. Olson, L.M. Wagner, A. Onar-Thomas, M. Kocak, R. J. Packer, S. Goldman, S. Gururangan, A. Gajjar, T. Demuth, L.E. Kun, J.M. Boyett, R.J. Gilbertson, Phase I trial of MK-0752 in children with refractory CNS malignancies: a pediatric brain tumor consortium study, *J. Clin. Oncol.* 29 (26) (2011) 3529–3534.
- [16] M.F. Weingart, J.J. Roth, M. Hutt-Cabezas, T.M. Busse, H. Kaur, A. Price, R. Maynard, J. Rubens, I. Taylor, X.G. Mao, J. Xu, Y. Kuwahara, S.J. Allen, A. Erdreich-Epstein, B.E. Weissman, B.A. Orr, C.G. Eberhart, J.A. Biegel, E. H. Raabe, Disrupting LIN28 in atypical teratoid rhabdoid tumors reveals the importance of the mitogen activated protein kinase pathway as a therapeutic target, *Oncotarget* 6 (5) (2015) 3165–3177.

- [17] M.H. Meel, M. Guillén Navarro, M.C. de Gooijer, D.S. Metselaar, P. Waranecki, M. Breur, T. Lagerweij, L.E. Wedekind, J. Koster, M.D. van de Wetering, N. Schouten-van Meeteren, E. Aronica, O. van Tellingen, M. Bugiani, T.N. Phoenix, G.J.L. Kaspers, E. Hulleman, MEK/MELK inhibition and blood-brain barrier deficiencies in atypical teratoid/rhabdoid tumors, *Neuro Oncol.* 22 (1) (2020) 58–69.
- [18] D. Popovski, A. Huang, Targeting MEK/MELK in atypical teratoid rhabdoid tumor: a treatment approach aimed at exploiting blood-brain barrier deficiencies, *Neuro Oncol.* 22 (1) (2020) 3–4.
- [19] S. Shahab, J. Rubens, H. Kaur, H. Sweeney, C.G. Eberhart, E.H. Raabe, MEK inhibition suppresses growth of atypical teratoid/rhabdoid tumors, *J. Neuropathol. Exp. Neurol.* 79 (7) (2020) 746–753.
- [20] E. Alva, J. Rubens, S. Chi, T. Rosenberg, A. Reddy, E.H. Raabe, A. Margol, Recent progress and novel approaches to treating atypical teratoid rhabdoid tumor, *Neoplasia* 37 (2023) 100880.
- [21] I. Alimova, D. Wang, E. Danis, A. Pierce, A. Donson, N. Serkova, K. Madhavan, S. Lakshmanachetty, I. Balakrishnan, N.K. Foreman, S. Mitra, S. Venkataraman, R. Vibhakar, Targeting the TP53/MDM2 axis enhances radiation sensitivity in atypical teratoid rhabdoid tumors, *Int. J. Oncol.* 60 (3) (2022).
- [22] I. Alimova, A.M. Pierce, P. Harris, A. Donson, D.K. Birks, E. Prince, I. Balakrishnan, N.K. Foreman, M. Kool, L. Hoffman, S. Venkataraman, R. Vibhakar, Targeting Polo-like kinase 1 in SMARCB1 deleted atypical teratoid rhabdoid tumor, *Oncotarget* 8 (57) (2017) 97290–97303.
- [23] A. Morin, C. Soane, A. Pierce, B. Sanford, K.L. Jones, M. Crespo, S. Zahedi, R. Vibhakar, J.M. Mulcahy Levy, Proteasome inhibition as a therapeutic approach in atypical teratoid/rhabdoid tumors, *Neurooncol. Adv.* 2 (1) (2020) vdaa051.
- [24] H.M. Tran, K.S. Wu, S.Y. Sung, C.A. Changou, T.H. Hsieh, Y.R. Liu, Y.L. Liu, M. L. Tsai, H.L. Lee, K.L. Hsieh, W.C. Huang, M.L. Liang, H.H. Chen, Y.Y. Lee, S.C. Lin, D.M. Ho, F.C. Chang, M.E. Chao, W. Chen, S.S. Chu, A.L. Yu, Y. Yen, C.C. Chang, T. Wong, Upregulation of protein synthesis and proteasome degradation confers sensitivity to proteasome inhibitor bortezomib in myc-atypical teratoid/rhabdoid tumors, *Cancers (Basel)* 12 (3) (2020).
- [25] Y. Nakano, M. Takadera, M. Miyazaki, Z. Qiao, K. Nakajima, R. Noguchi, R. Oyama, Y. Kimura, Y. Okuhiro, K. Yamasaki, N. Kunihiro, H. Fukushima, T. Inoue, J. Hara, T. Ozawa, T. Kondo, K. Ichimura, Drug screening with a novel tumor-derived cell line identified alternative therapeutic options for patients with atypical teratoid/rhabdoid tumor, *Hum. Cell* 34 (1) (2021) 271–278.
- [26] I. Paassen, J. Williams, C. Ríos Arceo, F. Ringnalda, K.S. Mercer, J.L. Buhl, N. Moreno, A. Federico, N.E. Franke, M. Kranendonk, S.A. Upadhyaya, K. Kerl, M. van de Wetering, H. Clevers, M. Kool, E.W. Hoving, M.F. Roussel, J. Drost, Atypical teratoid/rhabdoid tumoroids reveal subgroup-specific drug vulnerabilities, *Oncogene* 42 (20) (2023) 1661–1671.
- [27] A. Forget, L. Martignetti, S. Puget, L. Calzone, S. Brabetz, D. Picard, A. Montagud, S. Liva, A. Sta, F. Dingli, G. Arras, J. Rivera, D. Loew, A. Besnard, J. Lacombe, M. Pagès, P. Varlet, C. Dufour, H. Yu, A.L. Mercier, E. Indersie, A. Chivet, S. Leboucher, L. Sieber, K. Beccaria, M. Gombert, F.D. Meyer, N. Qin, J. Bartl, L. Chavez, K. Okonechnikov, T. Sharma, V. Thatikonda, F. Bourdeaut, C. Pouponnot, V. Ramaswamy, A. Korshunov, A. Borkhardt, G. Reifenberger, P. Pouillet, M.D. Taylor, M. Kool, S.M. Pfister, D. Kawauchi, E. Barillot, M. Remke, O. Ayrault, Aberrant ERBB4-SRC Signaling as a Hallmark of Group 4 Medulloblastoma Revealed by Integrative Phosphoproteomic Profiling, *Cancer Cell* 34 (3) (2018) 379–395.e7.
- [28] D. Capper, D.T.W. Jones, M. Sill, V. Hovestadt, D. Schrimpf, D. Sturm, C. Koelsche, F. Sahm, L. Chavez, D.E. Reuss, A. Kratz, A.K. Wefers, K. Huang, K.W. Pajtler, L. Schweizer, D. Stichel, A. Olar, N.W. Engel, K. Lindenberg, P.N. Harter, A. K. Braczynski, K.H. Plate, H. Dohmen, B.K. Garvalov, R. Coras, A. Hölsken, E. Hewer, M. Bewerunge-Hudler, M. Schick, R. Fischer, R. Beschorner, J. Schittenhelm, O. Staszewski, K. Wani, P. Varlet, M. Pages, P. Temming, D. Lohmann, F. Selt, H. Witt, T. Milde, O. Witt, P. Temming, E. Aronica, F. Giangaspero, E. Rushing, W. Scheurlen, C. Geisenberger, F.J. Rodriguez, A. Becker, M. Preusser, C. Haberler, R. Bjerkvig, J. Cryan, M. Farrell, M. Deckert, J. Hench, S. Frank, J. Serrano, K. Kannan, A. Tsirigos, W. Brück, S. Hofer, S. Brehmer, M. Seitz-Rosenhagen, D. Hänggi, V. Hans, S. Rozsnoi, J.R. Hansford, P. Kohlhof, B. W. Kristensen, M. Lechner, B. Lopes, C. Mawrin, R. Ketter, A. Kulozik, Z. Khatib, F. Heppner, A. Koch, A. Jouvet, C. Keohane, H. Mühlleisen, W. Mueller, U. Pohl, M. Prinz, A. Benner, M. Zapatka, N.G. Gottardo, P.H. Driever, C.M. Kramm, H. L. Müller, S. Rutkowski, K. von Hoff, M.C. Frühwald, A. Gnekow, G. Fleischhack, S. Tippelt, G. Calaminus, C.M. Monoranu, A. Perry, C. Jones, T.S. Jacques, B. Radlwimmer, M. Gessi, T. Pietsch, J. Schramm, G. Schackert, M. Westphal, G. Reifenberger, P. Wesseling, M. Weller, V.P. Collins, I. Blümcke, M. Bendszus, J. Debus, A. Huang, N. Jabado, P.A. Northcott, W. Paulus, A. Gajjar, G. W. Robinson, M.D. Taylor, Z. Jaunmuktane, M. Ryzhova, M. Platten, A. Unterberg, W. Wick, M.A. Karajannis, M. Mittelbronn, T. Acker, C. Hartmann, K. Aldape, U. Schüller, R. Buslei, P. Lichter, M. Kool, C. Herold-Mende, D.W. Ellison, M. Hasselblatt, M. Snuderl, S. Brandner, A. Korshunov, A. von Deimling, S. M. Pfister, DNA methylation-based classification of central nervous system tumours, *Nature* 555 (7697) (2018) 469–474.
- [29] M.A. Manavi, M.H. Fathian Nasab, R. Mohammad Jafari, A.R. Dehpour, Mechanisms underlying dose-limiting toxicities of conventional chemotherapeutic agents, *J. Chemother.* 36 (8) (2024) 623–635.
- [30] T.A. Baudino, Targeted cancer therapy: the next generation of cancer treatment, *Curr. Drug Discov. Technol.* 12 (1) (2015) 3–20.
- [31] R.D. Rao, J.C. Buckner, J.N. Sarkaria, Mammalian target of rapamycin (mTOR) inhibitors as anti-cancer agents, *Curr. Cancer Drug Targets* 4 (8) (2004) 621–635.
- [32] F. Ciardiello, R. Caputo, R. Bianco, V. Damiano, G. Pomato, S. De Placido, A. R. Bianco, G. Tortora, Antitumor effect and potentiation of cytotoxic drugs activity in human cancer cells by ZD-1839 (Iressa), an epidermal growth factor receptor-selective tyrosine kinase inhibitor, *Clin. Cancer Res.* 6 (5) (2000) 2053–2063.
- [33] P.Y. Wen, A. Stein, M. van den Bent, J. De Greve, A. Wick, F. de Vos, N. von Bubnoff, M.E. van Linde, A. Lai, G.W. Prager, M. Campone, A. Fasolo, J.A. Lopez-Martin, T.M. Kim, W.P. Mason, R.D. Hofheinz, J.Y. Blay, D.C. Cho, A. Gazzah, D. Pouessel, J. Yachnin, A. Boran, P. Burgess, P. Ilankumaran, E. Gasal, V. Subbiah, Dabrafenib plus trametinib in patients with BRAF(V600E)-mutant low-grade and high-grade glioma (ROAR): a multicentre, open-label, single-arm, phase 2, basket trial, *Lancet Oncol.* 23 (1) (2022) 53–64.
- [34] E. Bouffet, J.R. Hansford, M.L. Garré, J. Hara, A. Plant-Fox, I. Aerts, F. Locatelli, J. van der Lugt, L. Papusha, F. Sahm, U. Tabori, K.J. Cohen, R.J. Packer, O. Witt, L. Sandalic, A. Bento Pereira da Silva, M. Russo, D.R. Hargrave, Dabrafenib plus trametinib in pediatric glioma with BRAF V600 mutations, *N. Engl. J. Med.* 389 (12) (2023) 1108–1120.
- [35] E. Bouffet, B. Geoerger, C. Moertel, J.A. Whitlock, I. Aerts, D. Hargrave, L. Osterloh, E. Tan, J. Choi, M. Russo, E. Fox, Efficacy and safety of trametinib monotherapy or in combination with dabrafenib in pediatric BRAF V600-mutant low-grade glioma, *J. Clin. Oncol.* 41 (3) (2023) 664–674.
- [36] W.X. Mai, L. Gosa, V.W. Daniels, L. Ta, J.E. Tsang, B. Higgins, W.B. Gilmore, N. A. Bayley, M.D. Harati, J.T. Lee, W.H. Yong, H.I. Kornblum, S.J. Bensinger, P. S. Mischel, P.N. Rao, P.M. Clark, T.F. Cloughesy, A. Letai, D.A. Nathanson, Cytoplasmic p53 couples oncogene-driven glucose metabolism to apoptosis and is a therapeutic target in glioblastoma, *Nat. Med.* 23 (11) (2017) 1342–1351.
- [37] C. Tse, A.R. Shoemaker, J. Adickes, M.G. Anderson, J. Chen, S. Jin, E.F. Johnson, K. C. Marsh, M.J. Mitten, P. Nimmer, L. Roberts, S.K. Tahir, Y. Xiao, X. Yang, H. Zhang, S. Fesik, S.H. Rosenberg, S.W. Elmore, ABT-263: a potent and orally bioavailable Bcl-2 family inhibitor, *Cancer Res.* 68 (9) (2008) 3421–3428.
- [38] J.J. Hwang, J. Kuruvilla, D. Mendelson, M.J. Pishvaian, J.F. Deeken, L.L. Siu, M. S. Berger, J. Viallet, J.L. Marshall, Phase I dose finding studies of abatoclax (GX15-070), a small molecule pan-BCL-2 family antagonist, in patients with advanced solid tumors or lymphoma, *Clin. Cancer Res.* 16 (15) (2010) 4038–4045.
- [39] M. Badawi, R. Menon, A.E. Place, T. Palenski, G. Sunkersett, R. Arrendale, R. Deng, S.M. Federico, T.M. Cooper, A.H. Salem, Venetoclax penetrates the blood brain barrier: a pharmacokinetic analysis in pediatric leukemia patients, *J. Cancer* 14 (7) (2023) 1151–1156.
- [40] S.W. Ho, Y.T. Tsui, T.T. Wong, S.K. Cheung, W.B. Goggins, L.M. Yi, K.K. Cheng, L. Baum, Effects of 17-allylamino-17-demethoxygeldanamycin (17-AAG) in transgenic mouse models of frontotemporal lobar degeneration and Alzheimer's disease, *Transl. Neurodegener.* 2 (1) (2013) 24.
- [41] M.J. Egorin, E.G. Zuhowski, D.M. Rosen, D.L. Sentz, J.M. Covey, J.L. Eiseman, Plasma pharmacokinetics and tissue distribution of 17-(allylamino)-17-demethoxygeldanamycin (NSC 330507) in CD2F1 mice, *Cancer Chemother. Pharmacol.* 47 (4) (2001) 291–302.
- [42] K. Jhaveri, S. Modi, Ganetespib: research and clinical development, *Onco Targets Ther.* 8 (2015) 1849–1858.
- [43] J.W. Goldman, R.N. Raju, G.A. Gordon, I. El-Hariry, F. Teofilivici, V.M. Vukovic, R. Bradley, M.D. Karol, Y. Chen, W. Guo, T. Inoue, L.S. Rosen, A first in human, safety, pharmacokinetics, and clinical activity phase I study of once weekly administration of the Hsp90 inhibitor ganetespib (STA-9090) in patients with solid malignancies, *BMC Cancer* 13 (2013) 152.
- [44] S.A. Eccles, A. Massey, F.I. Raynaud, S.Y. Sharp, G. Box, M. Valenti, L. Patterson, A. de Haven Brandon, S. Gowen, F. Boxall, W. Aherne, M. Rowlands, A. Hayes, V. Martins, F. Urban, K. Boxall, C. Prodromou, L. Pearl, K. James, T.P. Matthews, K. M. Cheung, A. Kalusa, K. Jones, E. McDonald, X. Barril, P.A. Brough, J.E. Cansfield, B. Dymock, M.J. Drysdale, H. Finch, R. Howes, R.E. Hubbard, A. Surgenor, P. Webb, M. Wood, L. Wright, P. Workman, NVP-AUY922: a novel heat shock protein 90 inhibitor active against xenograft tumor growth, angiogenesis, and metastasis, *Cancer Res.* 68 (8) (2008) 2850–2860.
- [45] C.J. Burns, E. Fantino, I.D. Phillips, S. Su, M.F. Harte, P.E. Bukczynska, M. Frazzetto, M. Joffe, I. Kruszelnicki, B. Wang, Y. Wang, N. Wilson, R.J. Dilley, S. S. Wan, S.A. Charman, D.M. Shackelford, R. Fida, C. Malcontenti-Wilson, A. F. Wilks, CYT997: a novel orally active tubulin polymerization inhibitor with potent cytotoxic and vascular disrupting activity in vitro and in vivo, *Mol. Cancer Ther.* 8 (11) (2009) 3036–3045.
- [46] M. Burge, A.B. Francesconi, D. Kotasek, R. Fida, G. Smith, A. Wilks, P.A. Vasey, J. D. Lickliter, Phase I, pharmacokinetic and pharmacodynamic evaluation of CYT997, an orally-bioavailable cytotoxic and vascular-disrupting agent, *Invest. N. Drugs* 31 (1) (2013) 126–135.